







Lens-less fiber coupling of a 1550-nm mode-locked fiber laser light on a low-temperature-grown GaAs photoconductive antenna

TAKASHI OGURA,¹ YOSHIAKI NAKAJIMA,^{2,3}  YI-DA HSIEH,^{2,4} TAKEO MINAMIKAWA,^{2,4}  YASUHIRO MIZUTANI,^{2,5} HIROTSUGU YAMAMOTO,^{2,6} TETSUO IWATA,^{2,4} KAORU MINOSHIMA,^{2,3}  AND TAKESHI YASUI^{2,4,*} 

¹Graduate School of Advanced Technology and Science, Tokushima University, 2-1, Minami-Josanjima, Tokushima, Tokushima 770-8506, Japan

²JST, ERATO, MINOSHIMA Intelligent Optical Synthesizer Project, 2-1, Minami-Josanjima, Tokushima, Tokushima 770-8506, Japan

³Graduate School of Informatics and Engineering, The University of Electro-Communications, 1-5-1 Chofugaoka, Chofu, Tokyo 182-8585, Japan

⁴Graduate School of Technology, Industrial and Social Sciences, Tokushima University, 2-1, Minami-Josanjima, Tokushima, Tokushima 770-8506, Japan

⁵Graduate School of Engineering, Osaka University, 2-1, Yamadaoka, Suita, Osaka 565-0871, Japan

⁶Center for Optical Research and Education, Utsunomiya University, 7-1-2, Yoto, Utsunomiya, Tochigi 321-8585, Japan

*yasui.takeshi@tokushima-u.ac.jp

Abstract: A fiber-coupled photoconductive antenna (PCA) is a powerful tool for portable terahertz (THz) systems using a compact 1550-nm mode-locked Er:fiber laser with a fiber output port. However, a low-temperature-grown GaAs (LTG-GaAs) PCA could not be used for this purpose due to the need for wavelength conversion of the 1550-nm light, regardless of the good characteristics for PCA. In this article, we achieved the fiber coupling of the 1550-nm mode-locked fiber laser light on a bowtie-shaped LTG-GaAs PCA detector without the need for wavelength conversion. While the two-step photo-absorption mediated by midgap states in the LTG-GaAs PCA makes it possible to use the 1550-nm light, the similarity of the size between the PCA gap spacing and the fiber core diameter enables the direct contact coupling between the fiber output tip and the PCA gap without any optical components. The developed lens-less fiber-coupled LTG-GaAs PCA detector was effectively applied for the absolute frequency measurement of continuous-wave THz radiation based on the photo-carrier THz frequency comb. The combination of the lens-less fiber-coupled LTG-GaAs PCA with the compact 1550-nm fiber laser will be useful for the portable apparatus for the absolute frequency measurement of practical CW-THz sources and other applications.

© 2019 Optical Society of America under the terms of the [OSA Open Access Publishing Agreement](#)

1. Introduction

Photoconductive antenna (PCA) is a key component in terahertz (THz) technology and science because it can be used for both generation and detection of pulsed or continuous-wave (CW) THz radiation [1]. Low-temperature-grown GaAs (LTG-GaAs) PCA [2] has been widely used due to the high breakdown field, a subpicosecond carrier life-time, good mobility, low dark current noise, and good compatibility with laser sources around 800 nm, such as a mode-locked Ti:Sapphire laser or a frequency-doubled mode-locked Er:fiber laser. One drawback of this PCA is the optical band gap energy of 1.43 eV, corresponding to a wavelength of 867 nm, hindering

use of a 1550-nm mode-locked Er: fiber laser without the wavelength conversion. On the other hand, InGaAs PCA with lower band gap energy enables the direct excitation by a 1550-nm fiber laser light [3]. Furthermore, the direct coupling between the laser output and the PCA using an optical fiber benefits from portable, alignment-free, robust, and flexible measurement tools [4]. Regardless of these practical benefits, high dark current noise in InGaAs film hinders from replacing LTG-GaAs PCA with the fiber-coupled InGaAs PCA for compact THz systems using a 1550-nm mode-locked fiber laser. Several optical components for the free-space propagation and the wavelength conversion have been still used for the 1550-nm fiber laser at the sacrifice of practical benefits.

There has been an interesting report on the direct excitation of the LTG-GaAs PCA by the 1550-nm light, namely two-step photo-absorption mediated by midgap states in LTG-GaAs [5,6]. If such the direct excitation can be achieved under the fiber coupling between the 1550-nm laser light and the LTG-GaAs PCA, the advantage of the LTG-GaAs PCA will be combined with the practical benefits of the fiber-coupled InGaAs PCA. However, there are no attempts to do it because the tight focusing and the precise alignment of the 1550-nm light with an objective lens are required for the efficient excitation.

In this article, focusing on the fact that the gap spacing in PCA is comparable to the core diameter in a single-mode fiber, we achieved the lens-less fiber coupling of the 1550-nm light on a bowtie-shaped LTG-GaAs PCA detector, and applied it for the frequency measurement of CW-THz radiation based on the photo-carrier THz frequency comb (PC-THz comb) [7–12].

2. Results and discussion

2.1. Lens-less fiber coupling of a 1550-nm laser light on a bowtie-shaped LTG-GaAs PCA detector

We first investigated the efficiency of the photo-carrier generation in the two-step photo-absorption of LTG-GaAs PCA with the 1550-nm light by measuring the resistance of the antenna gap. The free-space-propagating output light from a mode-locked Er-doped fiber laser (Menlo Systems, C-Comb/P100; center wavelength $\lambda_c = 1550$ nm, pulse duration $\Delta\tau = 58$ fs, mean power $P_{mean} = 280$ mW) was focused onto the gap of a bowtie-shaped LTG-GaAs PCA detector (Hamamatsu Photonics, custom product, bowtie length = 1 mm, width = 5 μm , gap = 5 μm , carrier lifetime = 0.3 ps) with an objective lens (numerical aperture = 0.25). For comparison, we also evaluated the efficiency of photo-carrier generation in the same PCA by the 775-nm light, namely one-photon photo-absorption. To this end, the 1550-nm light was converted into the second-harmonic-generation (SHG) light at 775 nm ($\Delta\tau = 80$ fs) by a nonlinear optical crystal before focusing on the PCA gap with the same objective lens.

Figure 1 show a relationship between the incident laser power and the resistance of the PCA gap with respect to the 1550-nm light (red circle plots) and the 775-nm light (blue square plots). We confirmed a linear relation between them for both laser lights. However, the efficiency of the 1550-nm light was 10-time lower than that of the 775-nm light due to different mechanisms of photo-carrier generation. On the other hand, when the 1550-nm fiber laser light is used for the one-photon photo-absorption of the LTG-GaAs PCA at 775 nm, we have to consider the conversion efficiency of SHG light, which is typically around 10%. Since the total efficiency of two-step photo-absorption at 1550 nm is comparable to the combined efficiency of the SHG wavelength conversion and the one-photon photo-absorption at the 775-nm light, there is no significant difference between them in the signal efficiency. Figure 1 also reflects the relation between the measurement SNR of the f_{beat} signal discussed later and the illuminance of the PCA antenna.

Next, we directly coupled the 1550-nm laser light from the fiber tip onto the gap of a bowtie-shaped LTG-GaAs PCA detector without the use of the objective lens. To this end, we constructed a home-made, mode-locked Er-doped fiber laser ($\lambda_c = 1550$ nm, $\Delta\tau = 50$ fs, $P_{mean} = 150$ mW, f_{rep}

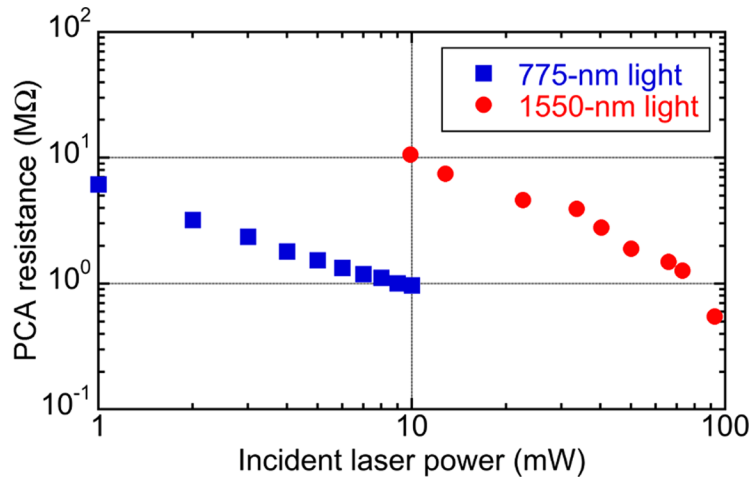


Fig. 1. Relationship between the input laser power and the PCA resistance with respect to the 1550-nm light and the 775-nm light.

$\approx 56,124,000$ Hz) [8]. All of them were housed in a 19-inch rack case for portable applications. The 1550-nm output light was delivered by a single-mode optical fiber (Corning SMF-28, core diameter = $8.2 \mu\text{m}$, clad diameter = $125 \mu\text{m}$). An inset of Fig. 2 shows the schematic diagram and the photograph of the lens-less fiber-coupled PCA. After removing a coating material from a single-mode fiber near the tip, the fiber tip was placed just in front of the PCA gap, and then its position was precisely adjusted to fit the 1550-nm light within the PCA gap using a 3-axis translation stage while monitoring the resistance of PCA. Finally, the configuration of the fiber tip to the PCA gap was fixed by the epoxy adhesive (curing time = 12 hours). We confirmed no change of PCA resistance ($< 1 \text{ M}\Omega$) before and after hardening of the adhesive. Even after lapse of more than several tens hours, the constant resistance was maintained due to the good mechanical stability at long time and no degradation of the adhesive.

2.2. Absolute frequency measurement of CW-THz radiation with lens-less fiber-coupled bowtie-shaped LTG-GaAs PCA detector

One interesting application of the lens-less fiber-coupled PCA is in the absolute frequency measurement of CW-THz radiation based on PC-THz comb [7–12] because the lens-less fiber-coupled PCA connected with the compact fiber laser will be useful for characterization of various CW-THz sources such as THz quantum cascade laser [13] and electronic CW-THz source [14]. Figure 2 shows the experimental setup of the absolute frequency measurement of CW-THz radiation. The principle of the operation in this system has been given in detail elsewhere [7,8,11]. Briefly described, the PC-THz comb is induced in the PCA for THz detection, namely PCA detector, by irradiation of the mode-locked laser light, and acts as a local oscillator with multiple known frequencies. When the CW-THz radiation is incident onto the PCA detector containing the PC-THz comb, the photoconductive mixing between the CW-THz radiation and the PC-THz comb modes generates a group of beat signals between them in RF region. In this case, the absolute frequency f_{THz} of CW-THz radiation is given by

$$f_{\text{THz}} = m f_{\text{rep}} \pm f_{\text{beat}} \quad (1)$$

where m is a mode number of PC-THz comb nearest in frequency to f_{THz} , f_{rep} is a laser repetition frequency, and f_{beat} is a beat frequency at the lowest frequency. To determine m and a sign of f_{beat} , we have to measure two f_{beat} values ($f_{\text{beat}1}$, $f_{\text{beat}2}$) corresponding two different f_{rep} values

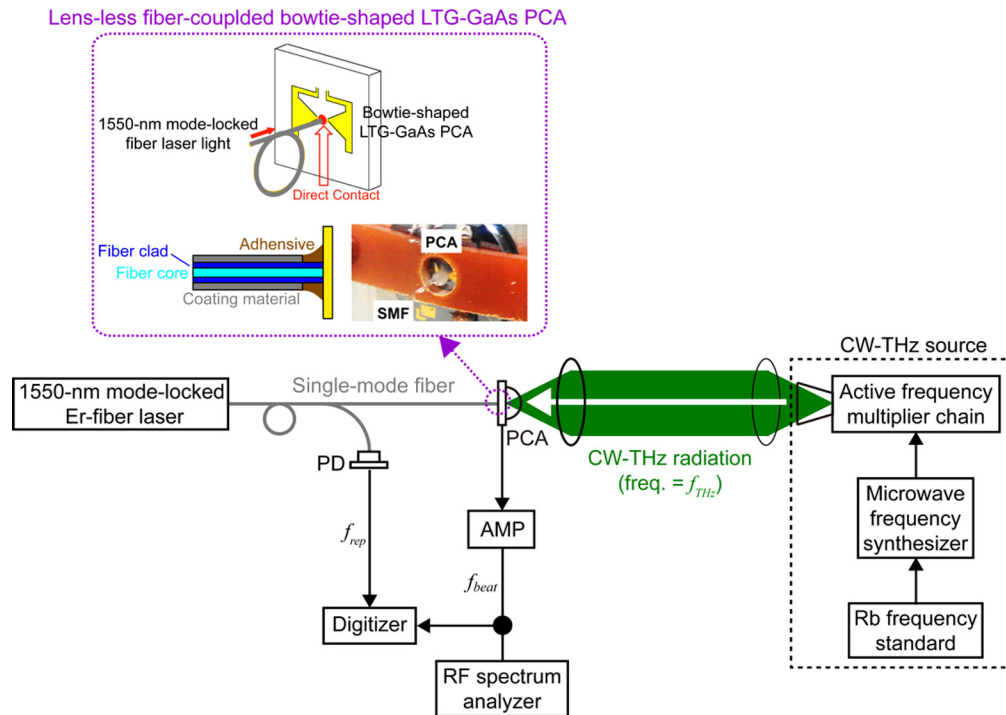


Fig. 2. Experimental setup for the absolute frequency measurement of CW-THz radiation based on the PC-THz comb. PCA: bowtie-shaped low-temperature-grown GaAs photoconductive antenna; AMP: current preamplifier. Inset shows the schematic diagram and the photograph of the lens-less fiber-coupled bowtie-shaped LTG-GaAs PCA.

(f_{rep1}, f_{rep2}) from the following equation.

$$f_{THz} = mf_{rep1} \pm f_{beat1} = mf_{rep2} \pm f_{beat2} \quad (2)$$

Finally, f_{THz} is determined by substituting them for m, f_{rep1} (or f_{rep2}), f_{beat1} (or f_{beat2}) in Eq. (2).

To evaluate the basic characteristics for this application, the lens-less fiber-coupled, bowtie-shaped LTG-GaAs PCA detector was applied for the absolute frequency measurement of an electronic CW-THz source (output frequency = 88,080,000,000 Hz, linewidth < 0.6 Hz, frequency stability = 5×10^{-11} at 1 s, frequency accuracy = 2×10^{-11} , average power = 2.5 mW), composed of an active frequency multiplier chain (Millitech AMC-10-R0000, multiplication factor = 6), a microwave frequency synthesizer (Agilent E8257D), and a rubidium frequency standard (Stanford Research Systems FS725), as shown in Fig. 2. The CW-THz radiation was focused onto the lens-less fiber-coupled LTG-GaAs PCA detector with a THz lens. The current signal from the LTG-GaAs PCA detector, namely the f_{beat} signal, was amplified by a current preamplifier (bandwidth = 40 MHz and transimpedance gain = 100,000 V/A). We first measured the RF spectrum of the f_{beat} signal with an RF spectrum analyzer (Agilent E4402B) because the high signal-to-noise ratio (SNR) of this signal is important in the correct determination of f_{THz} . Figure 3 shows the resulting RF spectrum of the f_{beat} signal (RBW = 1 kHz). The f_{beat} signal was obtained at SNR of 40 dB. This SNR was comparable to that in the free-space lens-coupled, bowtie-shaped LTG-GaAs PCA detector in the previous research [7,8], and hence is sufficient for the precise frequency measurement of f_{beat} .

Next, we demonstrated the real-time determination of f_{THz} in CW-THz radiation. To this end, the temporal waveforms for f_{rep} and f_{beat} were acquired simultaneously by a digitizer (resolution = 14

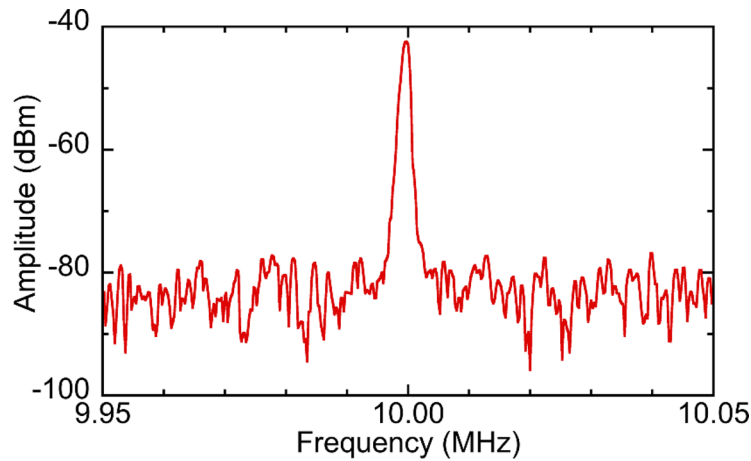


Fig. 3. RF spectrum of the f_{beat} signal (RBW = 1 kHz).

bit, sampling rate = 10 MHz) (see Fig. 2). From the acquired temporal waveforms, we obtained the instantaneous values of f_{rep} and f_{beat} at rate of 10 Hz by the instantaneous-frequency-calculation algorithm involving a Fourier transform (data length = 1,000,000), digital frequency filtering (bandpass width = 10 kHz), an inverse Fourier transform, a Hilbert transform, the time differential of the instantaneous phase, and the signal averaging [9]. In this demonstration, we measured f_{THz} in the frequency-fixed CW-THz radiation (freq. = 88,080,000,000 Hz). Figures 4(a) and 4(b) show the temporal changes of f_{rep} and f_{beat} , in which the f_{rep} value drifted to the lower frequency due to the free-running operation, whereas the f_{beat} value shifted to the higher frequency. Such opposite behavior of f_{rep} and f_{beat} indicated that the sign of f_{beat} was positive [see Fig. 4(c)]. The m value was calculated to be 1,569 during this data acquisition time by using two consecutive measurement values of f_{rep} and f_{beat} as f_{rep1} , f_{rep2} , f_{beat1} , and f_{beat2} in Eq. (2), respectively [11], as shown in Fig. 4(d). From these results, we determined the f_{THz} value at a measurement rate of 10 Hz as shown in Fig. 4(e). An inset of Fig. 4(e) shows the magnified fluctuation of f_{THz} from 0.1 s to 0.9 s. The mean and standard deviation of f_{THz} were 88,080,000,000.9 Hz and 4.6 Hz in 9 repetitive measurements of f_{THz} at a measurement rate of 10 Hz. Therefore, the accuracy and the precision of the absolute frequency measurement were 1.0×10^{-11} and 5.2×10^{-11} , respectively.

After 1 s, f_{THz} was suddenly changed from 88,080,000,000 Hz to 88,192,248,000 (see the green broken line in Fig. 4) so that the CW-THz radiation crossed 2 modes in PC-THz comb. Regardless of the mode-crossing behavior of the CW-THz radiation, the sign of f_{beat} , m , and f_{THz} were correctly determined. These results clearly demonstrated a high potential of the lens-less fiber-coupled LTG-GaAs PCA detector for the real-time, absolute frequency measurement of the CW-THz radiation.

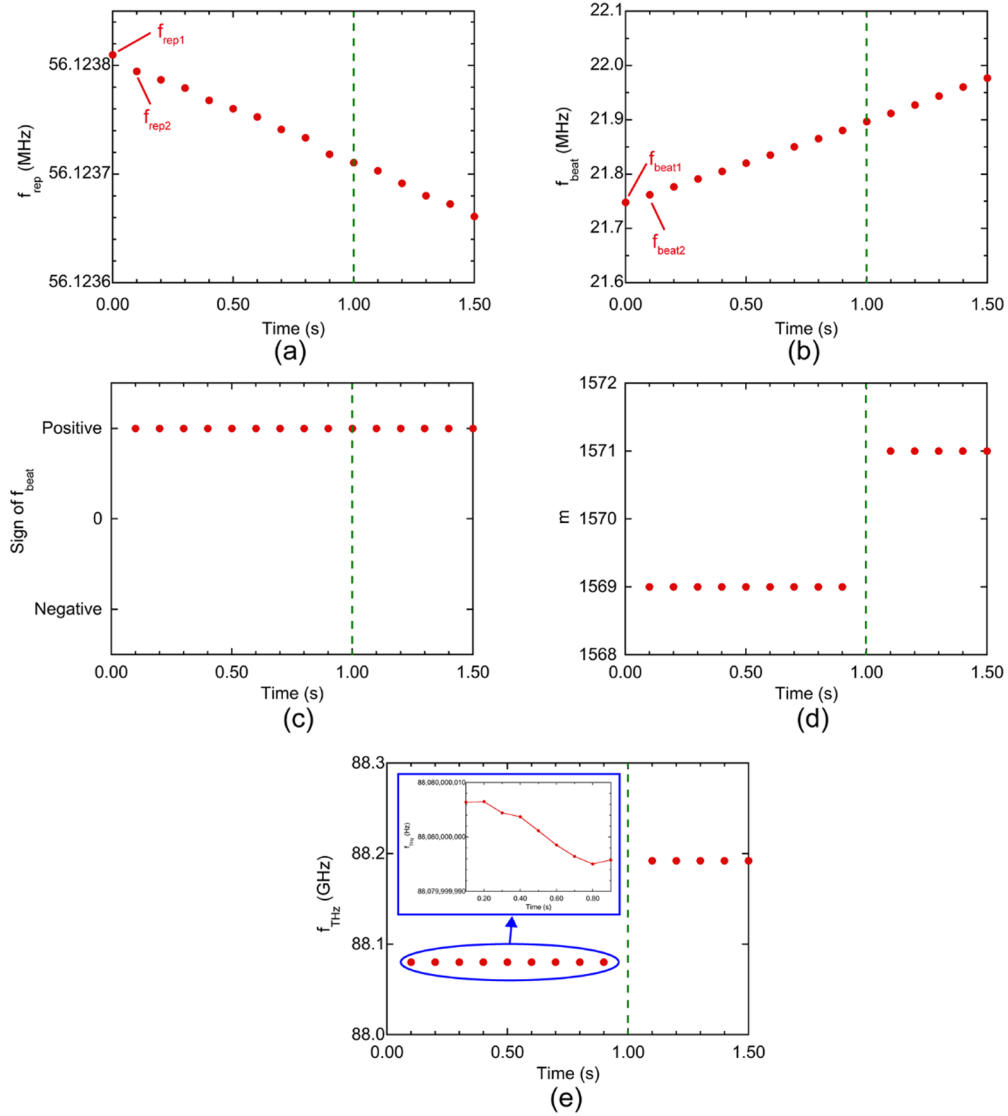


Fig. 4. Temporal changes of instantaneous values of (a) f_{rep} , (b) f_{beat} , (c) sign of f_{beat} , (d) m , and (e) f_{THz} for a measurement time of 1.5 s. The measurement rate was 10 Hz. Green broken line indicates the timing for the sudden change of f_{THz} from 88,080,000,000 Hz to 88,192,248,000 Hz.

3. Discussion

We here compared the proposed, lens-less fiber-coupled LTG-GaAs PCA detector with the commercially available, fiber-coupled InGaAs PCA detector. Both PCA detectors benefit from portable, alignment-free, robust, and flexible performance. Coupling efficiency of the 1550-nm light with the fiber-coupled LTG-GaAs PCA detector was lower than that of the 1550-nm light with the fiber-coupled InGaAs PCA detector due to the less efficient two-step photo-absorption mediated by midgap states in LTG-GaAs. This results in the requirement for several tens mW, 1550-nm light. However, one can get significant benefit of low dark current noise from use of LTG-GaAs PCA. From the comparison between the previous paper [8] and the present paper, THz detection efficiency of the proposed method is comparable to that of commercially available InGaAs PCA detector. Importantly from the viewpoint of practical use, the propose method is significantly cost-effective compared with the commercially available, fiber-coupled InGaAs PCA detector.

4. Conclusions

A single-mode fiber output port of a 1550-nm mode-locked Er: fiber laser light was coupled with a bowtie-shaped LTG-GaAs PCA detector without the needs for the wavelength conversion and the free-space optics. Since a core diameter of the single-mode fiber was just fitted within the PCA gap spacing, the tip of the fiber output port was directly contacted with the PCA gap for the two-step photo-absorption with the 1550-nm light. The less-less fiber-coupled LTG-GaAs PCA detector benefits the portable, alignment-free, robust, and flexible performance as well as the low dark current noise without the sacrifice of SNR because the efficiency of the two-step photo-absorption with the 1550-nm light was comparable to the combined efficiency of the SHG wavelength conversion and the one-photon photo-absorption with the 775-nm light. The effectiveness of the less-less fiber-coupled, bowtie-shaped LTG-GaAs PCA detector was demonstrated in the real-time absolute frequency measurement of the CW-THz radiation based on the PC-THz comb and its absolute frequency was determined with the frequency accuracy of 1.0×10^{-11} and the frequency precision of 5.2×10^{-11} . Although the bowtie-shaped LTG-GaAs PCA was used for the lens-less fiber coupling with the 1550-nm light in this article, it should be possible to make the lens-less fiber coupling with a dipole-shaped, or other shapes of LTG-GaAs PCA. The mechanical reinforcement of the lens-less fiber coupling is the future work for practical use of it. The combination of the lens-less fiber-coupled LTG-GaAs PCA detector with the compact 1550-nm fiber laser will be a powerful tool for portable applications, such as the characterization or calibration of practical CW-THz sources, dual-THz-comb spectroscopy with a single fiber laser [15,16], CW-THz radar [17].

Funding

Exploratory Research for Advanced Technology (ERATO) (JPMJER1304); Collaborative Research Based on Industrial Demand; Japan Science and Technology Agency (JST).

Acknowledgments

The authors wish to acknowledge Ms. Shoko Lewis of Tokushima Univ., Japan, for her help in preparation of the manuscript.

References

1. D. H. Auston, K. P. Cheung, and P. R. Smith, "Picosecond photoconducting Hertzian dipoles," *Appl. Phys. Lett.* **45**(3), 284–286 (1984).
2. M. Tani, S. Matsuura, K. Sakai, and S. Nakashima, "Emission characteristics of photoconductive antennas based on low-temperature-grown GaAs and semi-insulating GaAs," *Appl. Opt.* **36**(30), 7853–7859 (1997).

3. M. Suzuki and M. Tonouchi, "Fe-implanted InGaAs THz emitters for 1.56 μm wavelength excitation," *Appl. Phys. Lett.* **86**(5), 051104 (2005).
4. B. Sartorius, H. Roehle, H. Künzel, J. Böttcher, M. Schlak, D. Stanze, H. Venghaus, and M. Schell, "All-fiber terahertz time-domain spectrometer operating at 1.5 μm telecom wavelengths," *Opt. Express* **16**(13), 9565–9570 (2008).
5. M. Tani, K.-S. Lee, and X.-C. Zhang, "Detection of terahertz radiation with low-temperature-grown GaAs-based photoconductive antenna using 1.55 μm probe," *Appl. Phys. Lett.* **77**(9), 1396–1398 (2000).
6. J.-M. Rämmer, F. Ospald, G. von Freymann, and R. Beigang, "Generation and detection of terahertz radiation up to 4.5 THz by low-temperature grown GaAs photoconductive antennas excited at 1560 nm," *Appl. Phys. Lett.* **103**(2), 021119 (2013).
7. S. Yokoyama, R. Nakamura, M. Nose, T. Araki, and T. Yasui, "Terahertz spectrum analyzer based on a terahertz frequency comb," *Opt. Express* **16**(17), 13052–13061 (2008).
8. T. Yasui, R. Nakamura, K. Kawamoto, A. Ihara, Y. Fujimoto, S. Yokoyama, H. Inaba, K. Minoshima, T. Nagatsuma, and T. Araki, "Real-time monitoring of continuous-wave terahertz radiation using a fiber-based, terahertz-comb-referenced spectrum analyzer," *Opt. Express* **17**(19), 17034–17043 (2009).
9. H. Füsler, R. Judaschke, and M. Bieler, "High-precision frequency measurements in the THz spectral region using an unstabilized femtosecond laser," *Appl. Phys. Lett.* **99**(12), 121111 (2011).
10. H. Ito, S. Nagano, M. Kumagai, M. Kajita, and Y. Hanado, "Terahertz frequency counter with a fractional frequency uncertainty at the 10^{-17} level," *Appl. Phys. Express* **6**(10), 102202 (2013).
11. T. Minamikawa, K. Hayashi, T. Mizuguchi, Y.-D. Hsieh, D. G. Abdelsalam, Y. Mizutani, H. Yamamoto, T. Iwata, and T. Yasui, "Real-time determination of absolute frequency in continuous-wave terahertz radiation with a photocarrier terahertz frequency comb induced by an unstabilized femtosecond laser," *J. Infrared Millimeter Terahertz Waves* **37**(5), 473–485 (2016).
12. G. Hu, T. Mizuguchi, X. Zhao, T. Minamikawa, T. Mizuno, Y. Yang, C. Li, M. Bai, Z. Zheng, and T. Yasui, "Measurement of absolute frequency of continuous-wave terahertz radiation in real time using a free-running, dual-wavelength mode-locked, erbium-doped fibre laser," *Sci. Rep.* **7**(1), 42082 (2017).
13. M. Ravaro, C. Manquest, C. Sirtori, S. Barbieri, G. Santarelli, K. Blary, J.-F. Lampin, S. P. Khanna, and E. H. Linfield, "Phase-locking of a 2.5 THz quantum cascade laser to a frequency comb using a GaAs photomixer," *Opt. Lett.* **36**(20), 3969–3971 (2011).
14. D.-S. Yee, Y. Jang, Y. Kim, and D.-C. Seo, "Terahertz spectrum analyzer based on frequency and power measurement," *Opt. Lett.* **35**(15), 2532–2534 (2010).
15. G. Hu, T. Mizuguchi, R. Oe, K. Nitta, X. Zhao, T. Minamikawa, T. Li, Z. Zheng, and T. Yasui, "Dual terahertz comb spectroscopy with a single free-running fibre laser," *Sci. Rep.* **8**(1), 11155 (2018).
16. R. D. Baker, N. T. Yardimci, Y.-H. Ou, K. Kieu, and M. Jarrahi, "Self-triggered asynchronous optical sampling terahertz spectroscopy using a bidirectional mode-locked fiber laser," *Sci. Rep.* **8**(1), 14802 (2018).
17. T. Yasui, M. Fujio, S. Yokoyama, and T. Araki, "Phase-slope and phase measurements of tunable CW-THz radiation with terahertz comb for wide-dynamic-range, high-resolution, distance measurement of optically rough object," *Opt. Express* **22**(14), 17349–17359 (2014).